Available online at www.sciencedirect.com

ScienceDirect

Procedia Engineering 67 (2013) 279 – 287

Procedia Engineering

www.elsevier.com/locate/procedia

7th Asian-Pacific Conference on Aerospace Technology and Science, 7th APCATS 2013

Design of 10 kW Horizontal-Axis Wind Turbine (HAWT) Blade and Aerodynamic Investigation Using Numerical Simulation

C. J. Bai[1], F. B. Hsiao[2,*], M. H. Li[3], G. Y. Huang[4], Y. J. Chen[5]

[1,2,3,4,5]*Department of Aeronautics and Astronautics, National Cheng Kung University, No. 1, University Road, Tainan, 701, Taiwan*

Abstract

In this study, a horizontal-axis wind turbine (HAWT) blade with 10,000 Watt power output has been designed by the blade element momentum (BEM) theory and the modified stall model, and the blade aerodynamics are also simulated to investigate its flow structures and aerodynamic characteristics. The design conditions of the turbine blade in order to display the linear distributions of pitch angle in each section include the rated wind speed, design tip speed ratio and design angle of attack that have been set to 10 m/s, 6 and 6°, respectively. The turbine blade geometry was laid out using S822 airfoils and the blade aspect ratio is 8.02 divided into radius of 3 m and chord length of 0.374 m. Next, the improved BEM theory including Viterna-Corrigan stall model, tip-loss factor and stall delay model has been developed for predicting the performance of the designed turbine blade. Finally, the investigations of aerodynamic characteristics for the turbine blade were performed by the numerical simulation. The Reynolds averaged Navier-Stokes (RANS) equatios combined with the Spalart-Allmaras turbulence model that describes the three dimensional steady state flow on the wind turbine blade were solved with the aid of a commerical Computational Fluid Dynamic (CFD) code. A structured grid of approximately 2.4 million cells formulates the computational domain. The simulation results are compared with the improvd BEM theory at rated wind speed of 10 m/s and show that the CFD is a good method on aerodynamic invesigation of a HAWT blade.

Keywords: horizontal-axis wind turbine (HAWT), blade element momentum (BEM) theory, S822 airfoil, computational fluid dynamic (CFD)

Nomenclature

a	axial induction factor
a'	angular induction factor
C_l	lift coefficient

* Corresponding author.
E-mail address: fbhsiao@mail.ncku.edu.tw

doi:10.1016/j.proeng.2013.12.027

C_d	drag coefficient
C_T	thrust coefficient
C_{ave}	average chord length (m)
D	drag force (N)
F	tip loss factor
L	lift force (N)
N_b	number of blades
N_s	number of sections
P_{red}	rated power (W)
r	local radius (m)
R_e	radius of blade (m)
T_N	thrust (N)
T_Q	torque (N-m)
V	wind speed (m/s)
V_{rel}	rated wind speed (m/s)
Greek symbols	
φ	angle of relative wind (°)
θ_p	pitch angle (°)
α	angle of attack (°)
α_d	design angle of attack (°)
λ	tip speed ratio
λ_d	design tip speed ratio
ω	rotational speed (rad/s)
Subscripts	
i	number of sections
j	number of iterations

1. Introduction

In general, the sectional shape of the horizontal-axis wind turbine (HAWT) blade consists of the two-dimensional (2D) airfoils, which result the lift and drag forces by virtue of pressure differences across the 2D airfoil. Because of this, the blade element momentum (BEM) theory is widely used to outline a procedure for the aerodynamic design of a HAWT blade. The optimum distributions of the chord length and the pitch angle in each section can be acquired according to the design parameters, which include the rated wind speed, number of blades, design tip speed ratio and design angle of attack [1-4].

In recent years, many authors have performed the aerodynamic performance prediction of the HAWT blade using the simple BEM model [5,6]. In Ref. [5], the aerodynamic curves of lift and drag coefficients with the S809 airfoil between the angles of attack -30° and 90° at different Reynolds numbers have been characterized as the mathematical models in order to simply combine with the BEM model to predict the performance of NREL PHASE VI rotor. One of the most striking features of this problem is its lift and drag coefficients of the S809 airfoil in the stall region. The fact is that not all airfoils own the experimental data of lift and drag coefficients in the stall region for the mathematical model construction especially at the angles of attack between 30° to 90°. Ref. [6] also used the simple BEM model to develop the software tool for HAWT simulation. However, the study is limited in that it did not describe the aerodynamic data in the stall region for the different types of airfoils.

Computational Fluid Dynamic (CFD) is a good method for investigating the aerodynamic performance of different types of blade shape [1,3,7] such as Nation Aerospace Laboratory has successfully developed a wind turbine with 500kW, low-cost, horizontal-axis, two-bladed, downwind, teetered and stall regulated and used the CFD method on a consideration of optimum blade design and performance analysis [8]. In Ref. [9], authors have used the Reynolds Averaged Navier-Stokes (RANS) equations combined with the k-ω SST turbulence model that describes the three-dimensional (3D) steady state flow about the blade solved with the aid of a commercial CFD

code for computing the aerodynamic characteristics of the NREL Phase VI rotor blade which is a horizontal-axis downwind wind turbine rotor

2. Mathematical model

2.1. Turbine blade shape design

To begin with, there are several parameters needed to decide before the HAWT blade design shown in Tab. 1. Fig. 1 shows the forces and the angle of relative wind (φ), which consists of pitch angle (θ_p) and angle of attack (α), acting on a S822 airfoil in one of blade sections, where T_N and T_Q are defined as the normal (thrust) and tangential (torque) forces respectively, and both forces are generated by lift (L) and drag (D) forces. These angles and forces in each blade section can be obtained from the BEM theory, and further obtained the thrust and torque of the blade by the integration on all sections of blade. The angle of relative wind φ_i in each section is expressed as:

$$\varphi_i = \frac{2}{3}\tan^{-1}\left[\frac{1}{\lambda_d\left(\frac{r_i}{R}\right)}\right] \tag{1}$$

where λ_d is the design tip speed ratio, R is the radius of blade, r_i is the local radius of blade and subscript of i is the number of sections along the span-wise direction of blade. From Fig. 1, the pitch angle θ_p in each section is defined as:

$$\theta_{p,i} = \varphi_i - \alpha_d \tag{2}$$

where α_d is the design angle of attack. The average chord length $C_{ave.}$ in each section is expressed as:

$$C_{ave.,i} = \frac{8\pi r_i(1+\cos\varphi_i)}{N_b N_s C_{l,i,design}} \tag{3}$$

where N_b is the number of blades, N_s is the number of sections and $C_{l,i,design}$ is the lift coefficient at design angle of attack. The distributions of pitch angle and chord length along the blade are shown in Fig. 2.

Table 1. An example of a table

Name	Symbol	Value	Unit
Rated power	P_{red}	10000	watt
Rated wind speed	V_{red}	10	m/s
Radius of blade	R	3.0	m
Design tip speed ratio	λ_d	7	
Number of blades	N_b	3	
Design angle of attack	α_d	6	°

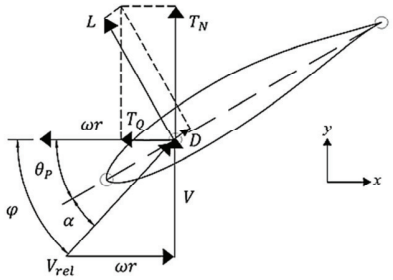

Fig. 1 Diagram of the angles and forces on one of sections of HAWT blade.

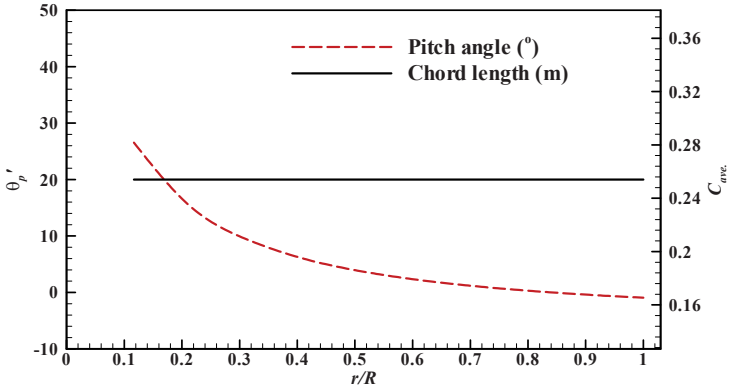

Fig. 2 Distributions of pitch angle and chord length in each section.

2.2. Aerodynamic performance prediction

The aerodynamic performance of HAWT blade can be solved from axial induction factor and angular induction factor by iterative method. There are six unknowns, angle of relative wind (φ), angle of attack (α), thrust coefficient (C_T), tip-loss factor (F), axis induction factor (a), and angular induction factor (a') needed to solve. The angle of relative wind is expressed as:

$$\varphi_{i,j} = \tan^{-1}\left[\frac{1-a_{i,j}}{\left(1+a'_{i,j}\right)\lambda_{r,i}}\right] \tag{4}$$

where λ_r is the local tip speed ratio and the subscript of j means the number of iterations. The angle of attack is expressed as:

$$\alpha_{i,j} = \varphi_{i,j} - \theta_{p_{i,j}} \tag{5}$$

where the values of θ_p can be found from Eqn. (2).

The method of cure fitting has been used to calculate the lift and drag coefficients ($C_{l,i,j}$, $C_{d,i,j}$) before stall angle of attack defined as:

$$C_{l,i,j} = C_{l0} + C_{l1}\alpha_{i,j} \tag{6}$$

$$C_{d,i,j} = C_{d0} + C_{d1}\alpha_{i,j} + C_{d2}\alpha_{i,j}^2 \tag{7}$$

where the C_{l0}, C_{l1}, C_{d0}, C_{d1} and C_{d2} are the local coefficients of lift and drag from the S822 airfoil at Reynolds number of 1×10^5 shown in Tab. 2(a) and Tab. 2(b). After the stall point, the VC stall model has been used to calculate the lift and drag coefficients.

$$C_{l,i,j} = C_{d,max}\sin2\left(\alpha_{i,j}\right) + K_L\cos^2(\alpha_{i,j})/\sin(\alpha_{i,j}) \tag{8}$$

$$C_{d,i,j} = C_{d,max}\sin^2(\alpha_{i,j}) + K_D\cos(\alpha_{i,j}) \tag{9}$$

where K_L and K_D are defined as:

$$K_L = \left[C_{l,s} - C_{d,max}\sin(\alpha_s)\cos(\alpha_s)\right]\frac{\sin(\alpha_s)}{\cos^2(\alpha_s)} \tag{10}$$

$$K_D = \frac{C_{d,s} - C_{d,max}\sin^2(\alpha_s)}{\cos(\alpha_s)} \tag{11}$$

where $C_{l,s}$ and $C_{d,s}$ are the lift and drag coefficient at the point of angle of attack (α_s) of 20° and $C_{d,max}$ depends on the aspect ratio (AR) as follows:

$$C_{d,max} = \begin{cases} 1.11 + 0.018AR, & AR \le 50 \\ 3.01, & AR > 50 \end{cases} \tag{12}$$

It is necessary to consider that in the state of rotating blade, the stall region initiates at the higher angle of attack as compared to wind tunnel experiment data on static airfoil. It has been characterized as centrifugal

pumping effects, which can reduce the adverse pressure gradient that leads to aerodynamic stall for an airfoil. A useful mathematical description of this effect based on the theoretical reasoning by laminar boundary layer theory can be written as:

$$C_{l,3D,i,j} = C_{l,i,j} + 3\left(\frac{C_{ave.,i}}{r_i}\right)^2 \Delta C_{l,i,j} \tag{13}$$

$$C_{d,3D,i,j} = C_{d,i,j} + 3\left(\frac{C_{ave.,i}}{r_i}\right)^2 \Delta C_{d,i,j} \tag{14}$$

where ΔC_l and ΔC_d are the difference between the lift and drag coefficients that can be obtained when the flow did not separate, and $C_{avg.,i}/r_i$ is the local chord normalized by the radial direction.

Table 2(a). The local lift coefficients of S822 airfoil for the Equation (6)

Reynolds number	Local lift coefficient	
Re	C_{l0}	C_{l1}
1×10^5	-0.006	0.1459

Table 2(b). The local drag coefficients of S822 airfoil for the Equation (7)

Reynolds number	Local drag coefficient		
Re	C_{d0}	C_{d1}	C_{d2}
1×10^5	0.00005	0.0002	0.0175

The tip loss factor which is described by Prandtl defined as:

$$F_{i,j} = \frac{2}{\pi}\cos^{-1}\left\{exp\left[-\left(\frac{N_b(1-r_i/R)}{2(r_i/R)\sin\varphi_{i,j}}\right)\right]\right\} \tag{15}$$

In the turbulent wake state, a solution can be found by using the empirical relationship between the axial induction factor and the thrust coefficient (C_T) which developed by Glauert [4,10], and the thrust coefficient is defined as:

$$C_{T,i,j} = \frac{\sigma_i(1-a_{i,j})^2 C_{l,3D,i,j}\cos\varphi_{i,j} + C_{d,3D,i,j}\sin\varphi_{i,j}}{\sin^2\varphi_{i,j}} \tag{16}$$

If $C_{T,i}$>0.96, then the axial induction factor is defined as:

$$a_{i,j} = \left(\frac{1}{F_{i,j}}\right)\left[0.143 + \sqrt{0.0203 - 0.6427(0.889 - C_{T,i,j})}\right] \tag{17}$$

While if C_T< 0.96 then the axial induction factor is solved by :

$$a_{i,j} = \frac{\left(C_{l,3D,i,j}\cos\varphi_{i,j} + C_{d,3D,i,j}\sin\varphi_{i,j}\right)\sigma_i}{4F_{i,j}\sin^2\varphi_{i,j} + \left(C_{l,3D,i,j}\cos\varphi_{i,j} + C_{d,3D,i,j}\sin\varphi_{i,j}\right)\sigma_i} \tag{18}$$

And then the angular inductor factor is defined as:

$$a'_{i,j} = \frac{C_{l,3D,i,j}\sin\varphi - C_{d,3D,i,j}\cos\varphi(1-a_{i,j})\sigma_i}{4F_{i,j}\lambda\sin^2\varphi_{i,j}} \tag{19}$$

By applying the Eqns. (3) to (19), it is possible to evaluate the torque, T_Q, and thrust, T_N, for each blade section and contains the correction factor of tip-loss factor and stall delay model as given in Eqn. (20):

$$T_{Q,i} = \sum_{i=1}^{N_s} 4F_{i,j}a'_{i,j}\left(1-a_{i,j}\right)\rho V\pi r_i^3\omega \Delta r \tag{20}$$

$$T_{N,i} = \sum_{i=1}^{N_s} 4F_{i,j}V^2 a_{i,j}\left(1 - a_{i,j}\right)\rho\pi r_i \,\Delta\, r \tag{21}$$

where V is the wind speed (m/s^2), ρ is the air density (kg/m^3) and Δr is the integrating factor, which has a relation including length between central hub to bladed tip (r_{tip}) and central hub to bladed root (r_{hub}), and the number of sections defined as $\triangle r$=(r_{tip}-r_{root})/N_s.

3. Numerical simulation

The mathematical model includes the continuity and momentum equations, which were solved in a Moving Reference Frame (MRF) that attached to the blades with the assumptions of incompressible and steady-state turbulent flow. Thus the continuity equation is written as:

$$\nabla(u_i) = 0 \tag{22}$$

The momentum equation is written as:

$$\rho\frac{\partial}{\partial X_j}\left(\overline{u_i u_j}\right) = -\left(\frac{\partial \bar{p}}{\partial X_i}\right) + \frac{\partial}{\partial X_j}\left(\overline{\tau_{ij}} - \overline{\rho u_i u_j}\right) \tag{23}$$

where p is the static pressure and τ_{ij} is the stress tensor.

In the present the turbulence in the boundary layer is modeled by the SST k-ω model and all computations are performed assuming the fully turbulent flow, excluding the laminar and transitional effects at the leading edge region of the blade.

$$\frac{\partial}{\partial t}(\rho k) + \frac{\partial}{\partial x_i}(\rho k u_i) = \frac{\partial}{\partial x_j}\left(\Gamma_k \frac{\partial}{\partial x_j}\right) + \widetilde{G_k} - Y_k + S_k \tag{24}$$

$$\frac{\partial}{\partial t}(\rho \omega) + \frac{\partial}{\partial x_i}(\rho \omega u_i) = \frac{\partial}{\partial x_j}\left(\Gamma_\omega \frac{\partial}{\partial x_j}\right) + \widetilde{G_\omega} - Y_\omega + S_\omega \tag{25}$$

where G_k is the generation of turbulence kinetic energy due to mean velocity gradient, G_ω is the generation of ω for modeling the turbulence production, Γ_k and Γ_ω are the effective diffusivity of k and ω, Y_k and Y_ω are the dissipation of k and ω due to turbulence for modeling the turbulence dissipation and D_ω is the cross diffusion term.

Now, the hub, tower and ground are neglected in the computational domain, that is a fair approximation for HAWT blade simulation. The computational domain is enclosed between a inner cylinder for MRF technique and an outer cylinder with radius equal to 6 times the blade radius measured from axial center. The flow field is extended to 8 blade radius along downwind direction and 1 radius along upwind direction. Exploiting the 120 degrees periodicity of the three-bladed and only one of the blades was simulated using MRF technique.

The Fluent's pro-processor Gambit was used to create the volume mesh, which is a hexahedral mesh of approximately 2.4 million cells. As shown in Fig. 3, the H-type grids are around the blade in order to resolve the boundary layer, the y+ values at wall are kept below 5 everywhere on the blade surface. All the calculations were carried out in an Intel Core 2 with 6 Gb Ram and the number of interations adjusted to reduce the scaled residual belowe the value of 10^{-5} which is the criterion of convergence.

The uniform wind speed profile 10 m/s is assumed at the inlet of the domain as boundary condition with fixed turbulence intensity and turbulence viscosity ratio and the working fluid for this simulation is the air with a density value of 1.25 kg/m^3. The boundary condition for the inner cylinder is Euler-slip and for the outer one is symmetry. Finally, the blade surface is assumed to the no-slip wall condition and the pressure outlet condition is assumed to the extreme surface of the downwind field.

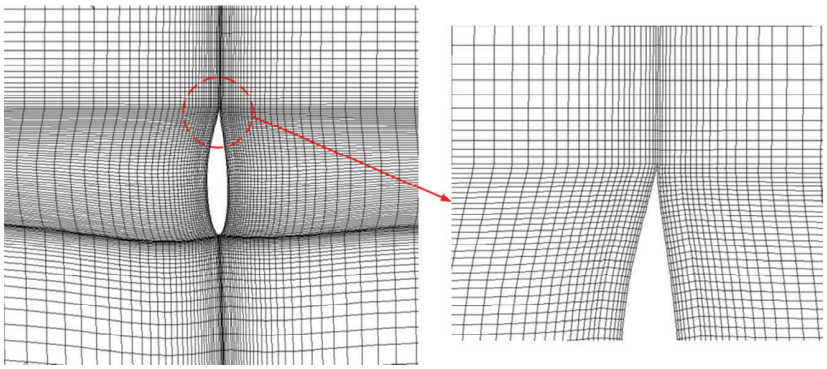

Fig. 3 H-type hexahedral mesh around sectional blade and left picture shows the detail of the mesh near the trailing edge of the blade

4. Results and discussion

The BEM theory has been successfully used to design a 10kW HAWT blade that included the optimum distributions of pitch angle and chord length in each section under the design point. The values of blade torque are obtained at 295 N-m and 271 N-m at wind speed of 10 m/s and tip speed ratio of 7.5 calculated by the improved BEM theory and the numerical simulation respectively. Fig. 4 and Fig. 5 show the torque (T_Q) and thrust (T_N) distributions in each blade section calculated by the improved BEM theory and further compared the results with the numerical simulation at wind speed of 10 m/s and tip speed ratio of 7.5. The values of T_Q from S_i/S of 0.5 to 0.9 have the same trends increasingly between the improved BEM and numerical simulation even though these have a lot of errors in this region. From the numerical simulation observation, the T_Q values are decreased from S_i/S of 0.8 to 1. It is evident that the tip-loss effect occurred at the blade tip region. It is also proven in Fig. 6, which displays the pressure distribution of the tested blade also at wind speed of 10 m/s and tip speed ratio of 7.5. It is shown that the vast pressure difference at S_i/S of 0.8 that is also conformed to Fig. 4. Fig. 5 shows the thrust (T_N) that has a good match between the improved BEM theory and the numerical simulation. It can be seen that the maximum thrust is about 140 N at S_i/S of 0.9 however calculated by the improved BEM and the numerical simulation. Fig. 7 displays the streamline over the blade section at r/R=90 %, r/R=51 % and r/R=21 %. Obviously, the flow behaviors are excellent at r/R=90 % and r/R=51 %. Oppositely, it has the stall phenomenon as the flow passed the blade section at r/R=21 %, which is at the region of blade root. So, it is can be proven that the torque distributions at blade tip region are larger than root region.

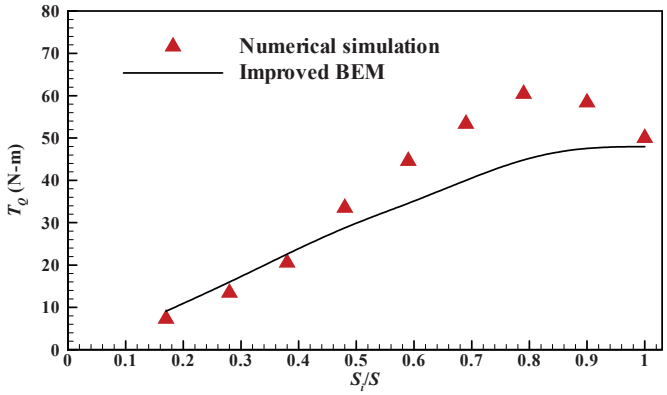

Fig. 4 Comparison of torques in each section between improved BEM and numerical simulation.

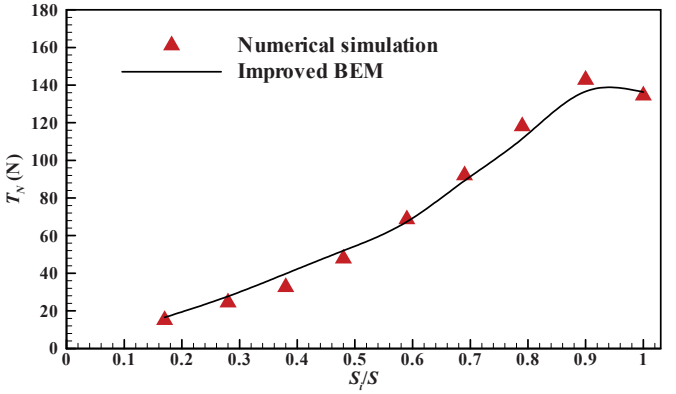

Fig. 5 Comparison of thrusts in each section between improved BEM and numerical simulation.

5. Conclusion

Consequently, the BEM theory is very successful in HAWT blade design. The modification factor and models were also combined into the BEM theory to predict the blade performance and there is a good comparison of torque and thrust in each section between the improved BEM theory and numerical simulation. The detailed flow fields were also investigated using fully 3D CFD simulations by means of the commercial code Fluent and the k-ω SST turbulence model and it has also showed that the Fluent package can be used to calculate the performances of a HAWT blade.

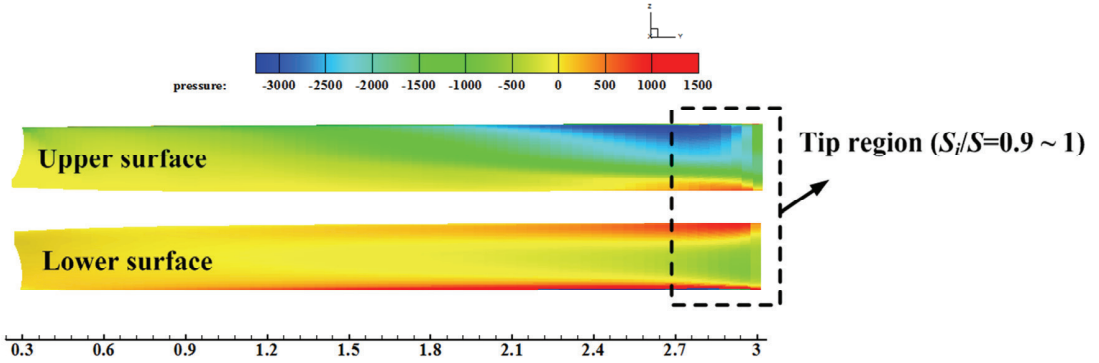

Fig. 6 Pressure distribution of blade at wind speed of 10 m/s and tip speed ratio of 7.5.

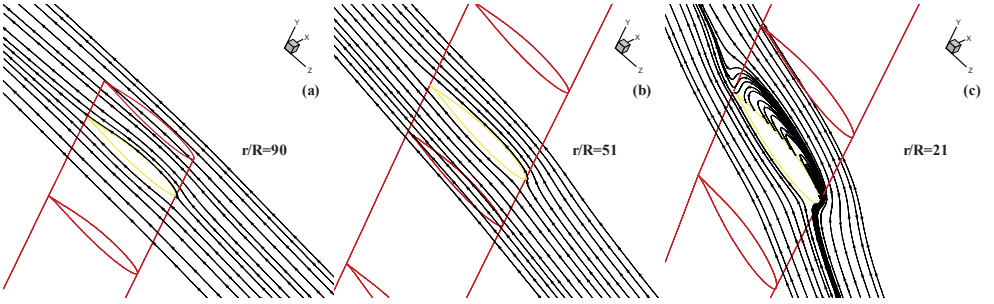

Fig. 7 The streamline plots at r/R=90 %, r/R=51 % and r/R=21 %.

Acknowledgements

This project was partially supported by the Nation Science Council of Taiwan through Grant NSC NSC 101-3113-E-006-003, and by National Cheng Kung University 6Y6M Grand D-102-23006 under Ministry of Education of Taiwan, which are greatly appreciated

References

[1] Hsiao, F. B., Bai, C. J., Chong, W. T., 2013. The Performance Test of Three Different Horizontal Axis Wind Turbine (HAWT) Blade Shapes Using Experimental and Numerical Methods, Energies, Vol. 6, pp. 2784-2803.
[2] Hsiao, F. B., Bai, C. J., 2013. Design and Power Curve Prediction of HAWT Blade by Improved BEM Theory, Accepted for publication in Journal of Chinese Society of Mechanical Engineers.
[3] Bai, C. J., Hsiao, F. B., 2010. "Code Development for Predicting the Aerodynamic Performance of a HAWT Blade with Variable-Speed Operation and Verification by Numerical Simulation," 17nd National Computational Fluid Dynamics (CFD) Conference. Taoyuan, Taiwan.
[4] Manwell, J. F., McGowan, J. G., and Rogers, A. L., 2009. Wind Energy Explained - Theory, Design and Application, John Wiley & Sons. Ltd, W. S., U. K.
[5] Lanzafame, R., Messina, M,. 2007. Fluid Dynamics Wind Turbine Design: Critical Analysis, Optimization and Application of BEM Theory, Renewable Energy 32, pp. 2291-2305.
[6] Vitale, A. J., Rossi, A. P., 2008. Software Tool for Horizontal-Axis Wind Turbine Simulation, International Journal of Hydrogen Energy 33, pp. 3460-3465.
[7] Bai, C. J., Hsiao, F. B., 2010. "Using CFD Computation for Aerodynamic Performance Design and Analysis of Horizontal Axis Wind Turbine Blade," 15nd National Computational Fluid Dynamics (CFD) Conference. Kaohsiung, Taiwan.
[8] Tachos, N. S., Filios, A. E., Margaris, D. P., Kaldellis, J. K. A., 2009. Computational Aerodynamics Simulation of the NREL Phase II Rotor, The Open Machanical Engineering Journal 3, pp. 9-6.
[9] Pape, A. L., Lecanu, J., 2004. 3D Navier-Stokes Computations of a Stall-regulated Wind Turbine, Wind Energy 7, pp. 309-324.
[10] Glauert, H., 1963. Airplane Propellers: Aerodynamic Theory, Dover Publications, New York.